2

Modeling Reservoir Rocks

Aquifers and natural petroleum reservoirs consist of a subvolume of sedimentary rocks that have sufficient porosity and permeability to store and transmit fluids. This chapter gives an overview of how such rocks are modeled, so as to become part of a simulation model. We start by describing briefly how sedimentary rocks and hydrocarbons are formed. In doing so, we introduce some geological concepts that you may encounter while working with subsurface modeling. We then move on to describe how rocks that contain hydrocarbons or aquifer systems are modeled in terms of a volumetric grid and a set of accompanying discrete petrophysical properties. Finally, we discuss how rock properties are represented in MRST, and show several examples of rock models with varying complexity, ranging from an idealized shoebox rock body with homogeneous properties, via the widely used SPE 10 model, to two realistic models, one synthetic and one representing a large-scale aquifer from the North Sea.

2.1 Formation of Sedimentary Rocks

Sedimentary rocks are created by mineral or organic particles that are deposited and accumulated on the Earth's surface or within bodies of water to create layer upon layer of sediments. The sedimentary rocks found in reservoirs come from sedimentary basins, inside which large-scale sedimentation processes have taken place. Sedimentary basins are formed as the result of stretching and breaking of the continental crust. As the crust is stretched, hot rocks deeper in the earth come closer to the surface. When the stretching stops, the hot rocks start to cool, which causes the crustal rock to gradually subside and move downward to create a basin. Such processes are taking place today. The Great Rift Valley of Africa is a good example of a so-called rift basin, where a rift splits the continental plate so that opposite sides of the valley are moving a millimeter apart each year. This gradually creates a basin inside which a new ocean may appear over the next hundred million years.

On the part of the Earth's surface that lies above sea level, wind and flowing water will remove soil and rock from the crust and transport it to another place where it is deposited when the forces transporting the mineral particles can no longer overcome gravity and friction. Mineral particles can also be transported and deposited by other geophysical

https://doi.org/10.1017/9781108591416.004 Published online by Cambridge University Press

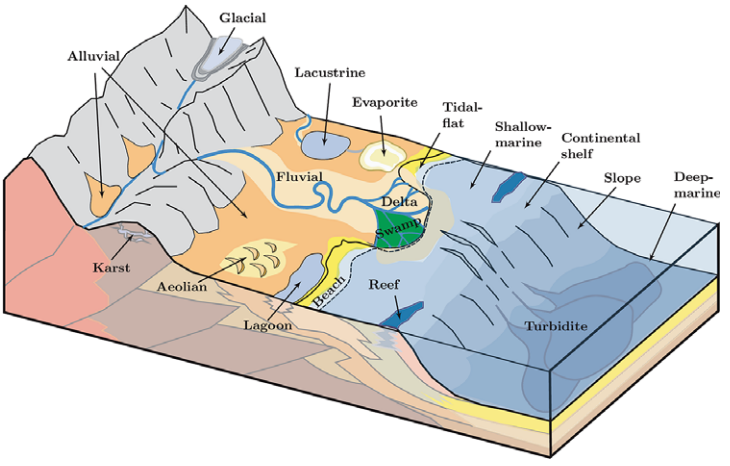

Figure 2.1 Illustration of various forms of depositional environments. Aeolian sediments are created by wind, evaporite minerals are left behind as water evaporates, fluvial sediments are deposited by rivers, and lacustrine sediments are deposited in lakes. Alluvial refers to the case where the geological process is not well described.

processes, like mass movement and glaciers. Over millions of years, layers of sediments will build up in deep waters, in shallow-marine waters along the coastline, or on land in lakes, rivers, sand deltas, and lagoons, see Figure 2.1. The sediments accumulate a depth of a few centimeters every one hundred years to form sedimentary beds (or strata) that may extend many kilometers in the lateral directions.

Over time, the weight of the upper layers of accumulating sediment will push the lower layers downward. A combination of heat from the Earth's center and pressure from the overburden will cause the sediments to undergo various chemical, physical, and biological processes (commonly referred to as diagenesis). These processes cause the sediments to consolidate so that the loose materials form a compact, solid substance that may come in varying forms. This process is called lithification. Sedimentary rocks have a layered structure with different mixtures of rock types with varying grain size, mineral types, and clay content. The composition of a rock depends strongly upon a combination of geological processes, the type of sediments that are transported, and the environment in which it is deposited. *Sandstone* are formed by mineral particles that are broken off from a solid material by weathering and erosion in a source area and transported by water to a place where they settle and accumulate. *Limestone* is formed by the skeletons of marine organisms such as corals, which have a high calcium content. Sandstone and limestone will typically contain relative large void spaces between mineral particles in which fluids can move easily. *Mudrocks*, on the other hand, are formed by compression of clay, mud, and silt, and will consist of relatively fine-grained particles. These rocks, which are sometimes also referred to as *shale*, will have small pores and therefore have limited ability to transmit

https://doi.org/10.1017/9781108591416.004 Published online by Cambridge University Press

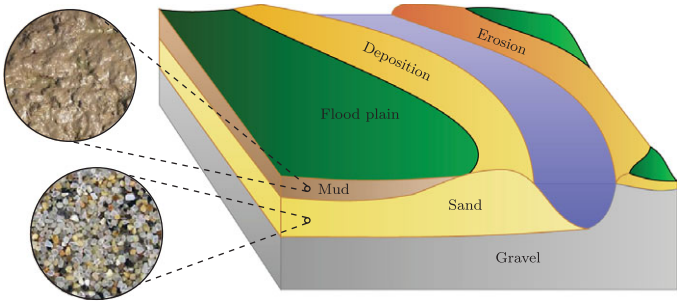

Figure 2.2 Illustration of a meandering river. Because water flows faster along the outer than along the inner curve of the bend, the river will erode along the outer bank and deposit at the inner bank. This causes the river to move sideways over time. Occasionally, the river will overflow its banks and cover the lower-lying flood plain with water and mud deposits that makes the soil fertile. Flood plains are therefore very important for agriculture.

fluids. Chemical rocks are formed by minerals that precipitate from a solution, e.g., salts that are left behind when oceans evaporate. Like mudrocks, salts are impermeable to fluids. Sediments will also generally contain organic particles that originate from the remains of plants, living creatures, and small organisms living in water.

To understand a particular rock formation, one must understand the prehistoric sedimentary environment from which it originates. It is common to distinguish between continental and marine environments. The primary source of sediments in a continental environment is rivers, inside which the moving water has high energy so that sediments will mainly be composed of fragments of preexisting minerals and rock, called clasts. Resulting rocks are therefore often referred to as *clastic rocks*. A flood plain is the area of the land adjacent to the river bank that will be covered by water when a river breaks its bank and floods during periods of high water discharge. Flood plains are created by bends in the river (meanders) that erode sideways; see Figure 2.2. A flood plain is the natural place for a river to diminish its kinetic energy. As the water moves, particles of rock are carried along by frictional drag of water on the particle, and water must flow at a certain velocity to suspend and transport a particle. Large particles are therefore deposited where the water flows rapidly, whereas finer particles will settle where the current is weak. River systems also create alluvial fans, which are fan-shaped sediment deposits built up by streams that carry debris from a single source. Other examples of continental environments are lagoons, lakes, and swamps that contain quiet water in which fine-grained sediments mingled with organic material are deposited.

For *marine rocks* formed in a sea or ocean, one usually makes the distinction between deep and shallow environments. In deep waters (200 m or more), the water moves relatively slowly over the bottom, and deposits will mainly consist of fine clay and skeletons of small microorganisms. However, if the sea bottom is slightly inclined, the sediments can become unstable and induce sudden currents of sediment-laden water to move rapidly downslope. These so-called turbidity currents are caused by density differences between the suspended

https://doi.org/10.1017/9781108591416.004 Published online by Cambridge University Press

sediments and the surrounding water and will generally be highly turbulent. Because of the high density, a turbidity current can transport larger particles than what pure water would be able to at the same velocity. These currents will therefore cause what can be considered as instantaneous deposits of large amounts of clastic sediments into deep oceans. The resulting rocks are called *turbidite*.

Shallow-marine environments are found near the coastline and contain greater kinetic energy caused by wave activity. Clastic sediments will therefore generally be coarser than in deep-marine environments and will consists of small-grained sand, clay, and silt that has been washed out and transported from areas of higher water energy on the continent. Far from the continent, the transport of clastic sediments is small, and deposits are dominated by biological activity. In warm waters, there are multitudes of small organisms that build carbonate skeletons, and, when deposited together with mud, these skeletons will turn into limestone, which is an example of a *carbonate rock*. Carbonate rocks can also be made from the skeletons of larger organisms living on coral reefs. Carbonates are soluble in slightly acidic water, and this may create *karst rocks* that contain large regions of void space (caves, caverns).

To model sedimentary rocks in a simulation model, one must be able to describe the geometry and the physical properties of different rock layers. A *bed* denotes the smallest unit of rock that is distinguishable from an adjacent rock layer unit above or below it, and can be seen as bands of different colors or textures in hillsides, cliffs, river banks, road cuts, etc. Each band represents a specific sedimentary environment, or mode of deposition, and can range from a few centimeters to several meters thick, often varying in the lateral direction. A sedimentary rock is characterized by its bedding, i.e., sequence of beds and lamina (less-pronounced layers). The bedding process is typically horizontal, but beds may also be deposited at a small angle, and parts of the beds may be weathered down or completely eroded away during deposition, allowing newer beds to form at an angle with older ones. Figure 2.3 shows two photos of sedimentary rock outcrops from Svalbard, which is one of the few places in Northern Europe where one can observe large-scale outcrops of sedimentary rocks. Figure 2.4 shows two more pictures of layered structures on meter to kilometer scale and centimeter scale, respectively.

Figure 2.3 Outcrops of sedimentary rocks from Svalbard, Norway. The length scale is a few hundred meters.

https://doi.org/10.1017/9781108591416.004 Published online by Cambridge University Press

Figure 2.4 Layered geological structures occur on both large and small scales in sedimentary rocks. The left picture is from Grand Canyon, the right picture is courtesy of Silje Støren Berg, University of Bergen.

Each sedimentary environment has its own characteristic deposits and forms what is called a *depositional facies*, i.e., a body of rock with distinct characteristics. Different sedimentary environments usually exist alongside each other in a natural succession. Small stones, gravel, and large sand particles are heavy and are deposited at the river bottom, whereas small sand particles are easily transported and are found at river banks and on the surrounding plains along with mud and clay. Following a rock layer of a given age, one will therefore see changes in the facies (rock type). Similarly, depositional environments change with time: shorelines move with changes in the sea level and land level or because of formation of river deltas, rivers change their course because of erosion or flooding, etc. Dramatic events like floods create more abrupt changes. At a given position, the accumulated sequence of beds will therefore contain different facies.

As time passes by, more and more sediments accumulate and the stack of beds piles up. Simultaneously, severe geological activity takes place: Cracking of continental plates and volcanic activity will change our eventual reservoir from a relatively smooth, layered sedimentary basin into a complex structure. Previously, continuous layers of sediments are compressed and pushed against each other to form arches, which are referred to as *anticlines*, and depressions, which are referred to as *synclines*. If the deposits contain large accumulations of salts, these will tend to flow upward through the surrounding layers to form large domes, since salts are lighter than other mineral particles. Likewise, as the sediments may be stretched, cut, shifted, or twisted in various directions, their movement may introduce fractures and faults. *Fractures* are cracks or breakage in the rock, across which there has been no movement. *Faults* are fractures or discontinuities in a volume of rock, across which movement in the crust has caused rock volumes on opposite sides to be displaced relative to each other. Some faults are small and localized, whereas others are part of the vast system of boundaries between tectonic plates that crisscrosses the crust of the Earth. Faults are described in terms of their *strike*, which is the compass direction in which the fault intersects the horizontal plane, and their *dip*, which is the angle that the fault plane makes with the horizontal, measured perpendicular to the strike. Faults are further classified

https://doi.org/10.1017/9781108591416.004 Published online by Cambridge University Press

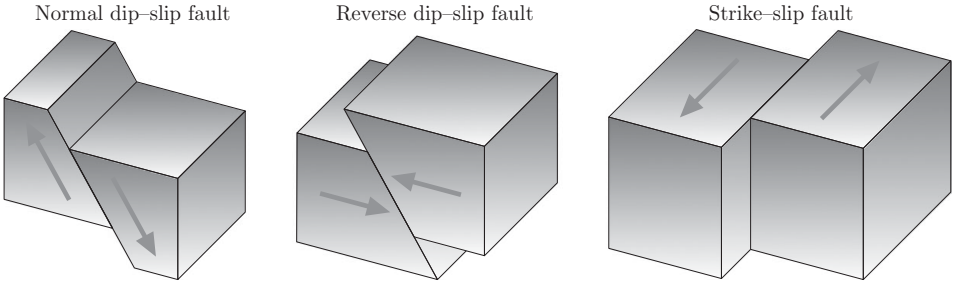

Figure 2.5 Fault types: In strike–slip faults, shear stress causes the rock volumes to slide past each other to the left and right in the lateral direction with very little vertical motion. In dip–slip faults, the rock volumes move predominantly in the vertical direction. A normal dip–slip fault occurs when the crust is extended and is sometimes called a divergent fault. Reverse dip–slip faults occur as a result of compressive shortening of the crust, and are sometimes called convergent faults, since rock volumes on opposite sides of the fault plane move horizontally toward one another.

by their *slip*, which is the displacement vector that describes the relative movement of rock volumes on opposite sides of the fault plane. The dip is usually separated into its vertical component, called *throw*, and its horizontal component, called *heave*. Figure 2.5 illustrates these different types of faults.

2.2 Creation of Crude Oil and Natural Gas

Deposits not only consist of sand grains, mud, and small rock particles, but will also contain remains of water-based plankton, algae, and other organisms that die and fall to the bottom where they are covered in mud. During their life, these organisms have absorbed heat from the sunlight and when they die and mix with the sediments, they take energy with them. As the sediments get buried deeper and deeper, the increasing heat from the Earth's core and pressure from the overburden will compress and "cook" the organic material that consists of cellulose, fatty oils, proteins, starches, sugar, waxes, and so on into an intermediate waxy product called kerogen. Whereas organic material contains carbon, hydrogen, and oxygen, the kerogen contains less oxygen and has a higher ratio of hydrogen to carbon. The maturation process that eventually turns kerogen into crude oil and natural gas depends highly upon temperature, and may take from a million years at 170°C to a hundred million of years at 100°C. Most of the oil and natural gas we extract today has been formed from the remains of prehistoric algae and zooplankton living in the ocean. Coal, on the other hand, is formed from the remains of dead plants. The rock in which this "cooking" process takes place is commonly referred to as the source rock. The chances of forming a source rock containing a significant amount of oil and gas increases if there has been an event that caused mass death of microorganisms in an ocean basin.

Pressure from sediments lying above the source rock will force the hydrocarbons to migrate upward through the void space in these newer sediments. The lightest hydrocarbons

https://doi.org/10.1017/9781108591416.004 Published online by Cambridge University Press

(methane and ethane) that form natural gas usually escape quickly, while the liquid oils move more slowly toward the surface. In this process, the natural gas will separate from the oil, and the oil will separate from the resident brine (salty water). At certain sites, the migrating hydrocarbons will be collected and trapped in structural or stratigraphic traps. Structural traps are created by tectonic activity that forms layers of sediments into anticlines, domes, and folds. Stratigraphic traps form because of changes in facies (e.g., in clay content) within the bed itself or when the bed is sealed by an impermeable layer such as mudstone, which consists of small and densely packed particles, and thus has strong capillary forces that cannot easily be overcome by the buoyancy forces that drive migrating hydrocarbons upward. If a layer of mudstone is folded into an anticline above a more permeable sandstone or limestone, it will therefore act as a caprock that prevents the upward migration of hydrocarbons. Stratigraphic traps are especially important in the search for hydrocarbons; approximately 4/5 of the world's oil and gas reserves are found in anticlinal traps.

Figure 2.6 illustrates the various forms in which migrating oil and natural gas can be trapped and accumulate to form petroleum reservoirs. *Anticlines* are typically produced when lateral pressure causes strata to fold, but can also result from draping and subsequent compaction of sediments accumulating over local elevations in the topography. *Stratigraphic traps* accumulate hydrocarbons because of changes in the rock type. For example, sand banks deposited by a meandering river is later covered by mud from the flood plain. Similarly, stratigraphic traps can form when rock layers are tilted and eroded away and subsequently covered by other low-permeable strata. *Fault traps* are formed when strata are moved in opposite directions along a fault line so that permeable rocks come in contact with impermeable rocks. The fault itself can also be an effective trap if it contains clays that

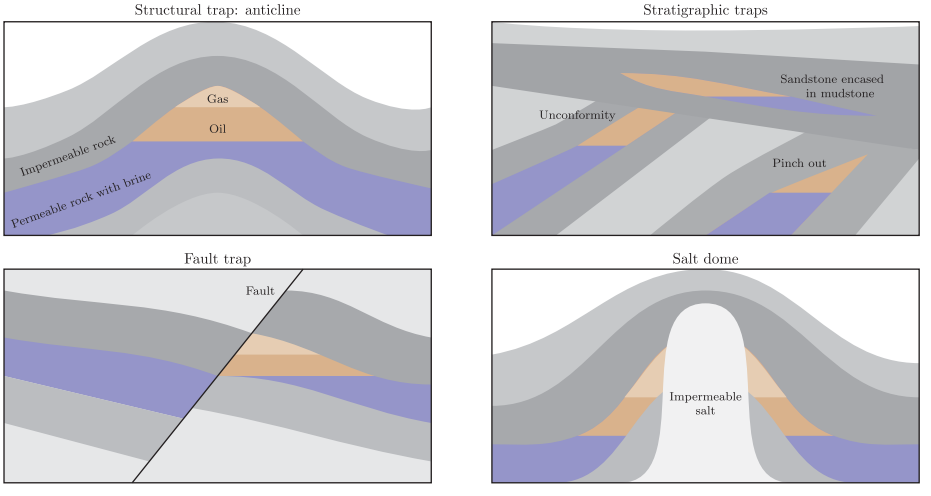

Figure 2.6 Various forms of traps in which migrating hydrocarbons can accumulate.

https://doi.org/10.1017/9781108591416.004 Published online by Cambridge University Press

are smeared as the layers of rock move past each other. *Salt domes* are created by buried salt deposits that rise unevenly through the surrounding strata. Oil can either rest against the salt itself, or the salt induces chemical reactions in the surrounding rock that makes it impermeable.

The first evidence of hydrocarbons beneath the earth's surface were found in so-called seeps, which are found in many areas throughout the world. Seeps are formed when the seal above a trap is breached so that oil and gas can migrate all the way through the geological layers and escape to the surface. As the hydrocarbons break through the surface, the lighter components will continue to escape to the atmosphere and leave behind heavier products like bitumen, pitch, asphalt, and tar have been exploited by mankind since paleolithic times. In 1859, Edwin L. Drake, also known as Colonel Drake, drilled the world's first exploration well into an anticline in Titusville, Pennsylvania to find oil 69.5 ft below the surface. Since then, an enormous amount of wells have been drilled to extract oil from onshore reservoirs in the Middle East, North America, etc. Drilling of submerged oil wells started just before the turn of the nineteenth century: from platforms built on piles in the fresh waters of Grand Lake St. Marys (Ohio) in 1891, and from piers extending into the salt water of the Santa Barbara Channel (California) in 1896. Today, hydrocarbons are recovered from offshore reservoirs that are located thousands of meters below the sea bed and in waters with a depth up to 2,600 m in the Gulf of Mexico, the North Sea, and offshore from Brazil.

2.3 Multiscale Modeling of Permeable Rocks

All sedimentary rocks consist of a solid matrix with an interconnected void. The void pore space allows the rocks to store and transmit fluids. The ability to store fluids is determined by the volume fraction of pores (*rock porosity*), and the ability to transmit fluids (*rock permeability*) is given by the interconnection of the pores.

Rock formations found in natural petroleum reservoirs are typically heterogeneous at all length scales, from the micrometer scale of pore channels between the solid particles making up the rock to the kilometer scale of a full reservoir formation. On the scale of individual grains, there can be large variation in grain sizes, giving a broad distribution of void volumes and interconnections. Moving up the scale, laminae may exhibit large contrasts on the mm–cm scale in the ability to store and transmit fluids because of alternating layers of coarse and fine-grained material. Laminae are stacked to form beds, which are the smallest stratigraphic units. The thickness of beds varies from millimeters to tens of meters, and different beds are separated by thin layers with significantly lower permeability. Beds are, in turn, grouped and stacked into parasequences or sequences (parallel layers that have undergone similar geologic history). Parasequences represent the deposition of marine sediments, during periods of high sea level, and tend to be somewhere in the range from 1 to 100 m thick and have a horizontal extent of several kilometers.

The trends and heterogeneity of parasequences depend on the depositional environment. For instance, whereas shallow-marine deposits may lead to rather smoothly varying

https://doi.org/10.1017/9781108591416.004 Published online by Cambridge University Press

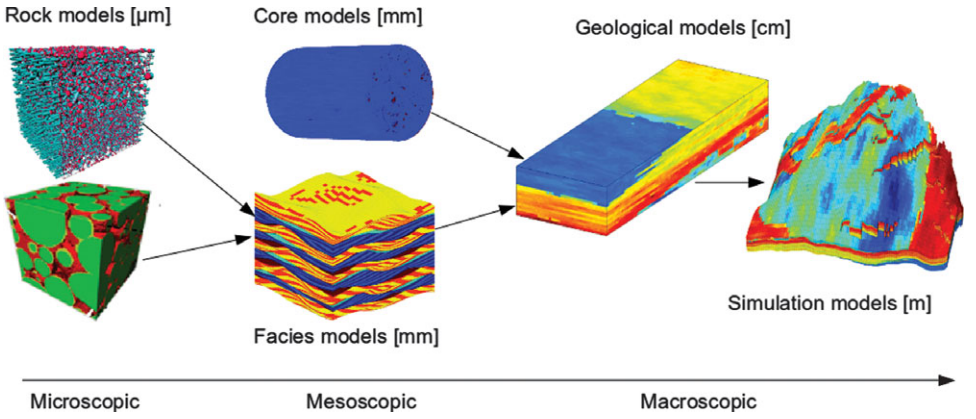

Figure 2.7 Illustration of the hierarchy of flow models used in subsurface modeling. The length scales are the vertical sizes of typical elements in the models.

permeability distributions with correlation lengths in the order of 10–100 m, fluvial reservoirs may contain intertwined patterns of sand bodies on a background with high clay content; see Figure 2.12. The reservoir geology can also consist of other structures such as shale layers (impermeable clays), which are the most abundant sedimentary rocks. Fractures and faults, on the other hand, are created by stresses in the rock and may extend from a few centimeters to tens or hundreds of meters. Faults may have a significantly higher or lower ability to transmit fluids than the surrounding rocks, depending upon whether the void space has been filled with clay material.

All these different length scales can have a profound impact on fluid flow. However, it is generally not possible to account for all pertinent scales that impact the flow in a single model. Instead, one has to create a hierarchy of models for studying phenomena occurring at reduced spans of scales. This is illustrated in Figure 2.7. Microscopic models represent the void spaces between individual grains and are used to provide porosity, permeability, electrical, and elastic properties of rocks from core samples and drill cuttings. Mesoscopic models are used to upscale these basic rock properties from the mm–cm scale of internal laminations, through the lithofacies scale (∼50 cm), to the macroscopic facies association scale (∼100 m) of geological models. In this book, we will primarily focus on another scale, simulation models, which represent the last scale in the model hierarchy. Simulation models are obtained by upscaling geological models and are either introduced out of necessity because geological models contain more details than a flow simulator can cope with, or out of convenience to provide faster calculation of flow responses.

2.3.1 Geological Characterization

To model a reservoir on a macroscopic scale, we basically need to represent its geology at a level of detail that is sufficient for the purpose the model is built to serve: to visualize how

https://doi.org/10.1017/9781108591416.004 Published online by Cambridge University Press

different experts perceive the reservoir, to provide estimates of hydrocarbon volumes, to assist well planning and geosteering, or as input to geophysical analysis (seismic modeling, rock mechanics) or flow simulations. For flow simulation, which is our primary concern in this book, we need a volumetric description that decomposes the reservoir into a set of grid cells (small 3D polygonal volumes) that are petrophysically and/or geometrically distinct from each other. With a slight abuse of terminology, we will refer to this as the *geological model*, which we distinguish from models describing the reservoir fluids and the forces that cause their movement.

Geological models are generally built in a sequence of steps, using a combination of stratigraphy (the study of rock layers and layering), sedimentology (study of sedimentary rocks), structural geology (the study of how rock layers are deformed over time by geological activity), diagenesis (the study of chemical, physical, and biological processes that transform sediments to rock), and interpretation of measured data. The starting point is usually a seismic interpretation, from which one obtains a representation of faults and geological horizons that bound different geological units. The seismic interpretation is used alongside a conceptual model in which geologists express how they believe the reservoir looks like based on studies of geological history and geological outcrops. The result can be expressed as a geometric model that consists of vertical or inclined surfaces representing faults, and horizontal or slightly sloping surfaces representing horizons that subdivide the reservoir volume into different geological units (zones). This zonation is obtained by combining seismic interpretation that describes the gross geometry of the reservoir with stratigraphic modeling and thickness information (isochores) obtained from well logs that define the internal layering. Once a model of the structural and stratigraphic architecture of the reservoir is established, the surface description can be turned into a 3D grid that is populated with cell and face properties that reflect the geological framework.

Unfortunately, building a geological model for a reservoir is like finishing a puzzle with most of the pieces missing. The amount of data available is limited due to the costs of acquiring it, and the data that is obtained is measured on scales that may be quite disparate from the geological features one needs to model. Seismic surveys give a sort of X-ray image of the reservoir, but are both expensive and time-consuming and can only give limited resolution; you cannot expect to see structures thinner than ten meters from seismic data. Information on finer scales is available from various measuring tools lowered into the wells to gather information of the rock in near-well region, e.g., by radiating the reservoir and measuring the response. Well logs have quite limited resolution, rarely down to centimeter scale. The most detailed information is available from rock samples (cores) extracted from the well. The industry uses X-ray, CT scan, as well as electron microscopes to gather high-resolution information from the cores, and the data resolution is only limited by the apparatus at hand. However, information from cores and well logs can only tell you how the rock looks like near the well, and extrapolating this information to the rest of the reservoir is subject to great uncertainty. Moreover, due to high costs, one cannot expect well logs and cores to be taken from every well. All these techniques give separately small contributions that can help build a geological model. However, in the end we still have very

https://doi.org/10.1017/9781108591416.004 Published online by Cambridge University Press

limited information available, considering that a petroleum reservoir can have complex geological features that span across all types of length scales from a few millimeters to several kilometers.

In summary, the process of making a geological model is generally strongly underdetermined. It is therefore customary to use a combination of deterministic and probabilistic modeling to estimate the subsurface characteristics between the wells. Deterministic modeling is used to specify large-scale structures such as faults, correlation, trends, and layering, which are used as input and controls to *geostatistical* techniques [258, 57, 82] that build detailed grid models satisfying statistical properties assumed for the petrophysical heterogeneity. In recent years, process models that seek to mimic deposition and subsequent structural changes have also gained more popularity since they tend to produce less artifacts in the geocellular models. Trends and heterogeneity in petrophysical properties depend strongly on the structure of sedimentary deposits, and high-resolution petrophysical realizations are thus rarely not built directly. Instead, one starts by building a *rock model* that is based on the structural model and consists of a set of discrete rock bodies (facies) that are specified to improve petrophysical classification and spatial shape. For carbonates, the modeled facies are highly related to diagenesis, while the facies modeled for sandstone reservoirs are typically derived from the depositional facies. By supplying knowledge of the depositional environment (fluvial, shallow-marine, deep-marine, etc.) and conditioning this to observed data, one can determine the geometry of the facies and how they are mixed.

To populate the modeled facies with petrophysical properties, it is common to replace the facies with a volumetric grid, and use stochastic simulation to generate multiple discrete realizations of the petrophysical properties defined on this grid. Each grid model has a plausible heterogeneity and can contain millions of cells. The collection of all realizations gives a measure of the uncertainty involved in the modeling. Hence, if the sample of realizations (and the upscaling procedure that converts the geological models into simulation models) is unbiased, then it is possible to supply predicted production characteristics, such as the cumulative oil production, obtained from simulation studies with a measure of uncertainty.

You can find a lot more details about the complex process of characterizing a reservoir and making geological models in the excellent textbook by Ringrose and Bentley [265]. The rest of this section will first introduce the concept of representative elementary volumes, which underlies the continuum models used to describe subsurface flow and transport, and then briefly discuss microscopic and mesoscopic modeling. This discussion is not essential to understand what follows in the next few chapters, and if you are not interested, you can therefore safely skip to Section 2.4, which discusses macroscopic modeling of reservoir rocks.

2.3.2 Representative Elementary Volumes

Choosing appropriate modeling scales is often done by intuition and experience, and it is hard to give general guidelines. An important concept in choosing model scales is the

https://doi.org/10.1017/9781108591416.004 Published online by Cambridge University Press

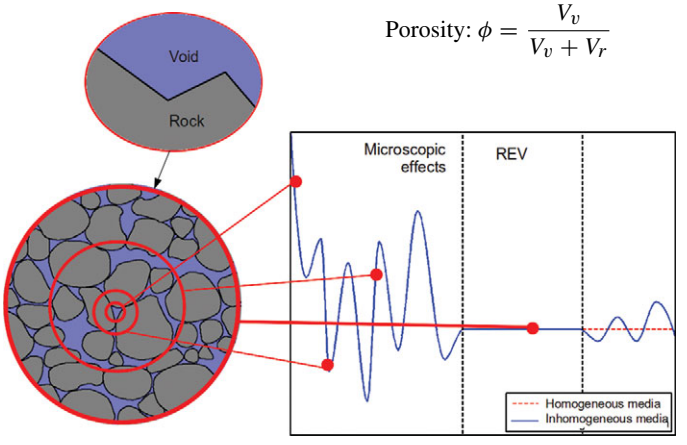

Figure 2.8 The concept of a representative elementary volume (REV), here illustrated for porosity, which measures the fraction of void space to bulk volume.

notion of representative elementary volumes (REVs), which is the smallest volume over which a measurement can be made and be representative of the whole. This concept is based on the idea that petrophysical flow properties are constant on some intervals of scale; see Figure 2.8. Representative elementary volumes, if they exist, mark transitions between scales of heterogeneity, and present natural length scales for modeling.

To identify a range of length scales where REVs exist, e.g., for porosity, we move along the length-scale axis from the micrometer-scale of pores toward the kilometer-scale of the reservoir. At the pore scale, the porosity is a rapidly oscillating function equal to zero (in solid rock) or to one (in the pores). Hence, obviously no REVs can exist at this scale. At the next characteristic length scale, the core scale level, we find laminae deposits. Because the laminae consist of alternating layers of coarse and fine grained material, we cannot expect to find a common porosity value for the different rock structures. Moving further along the length-scale axis, we may find long thin layers, perhaps extending throughout the entire horizontal length of the reservoirs. Each of these individual layers may be nearly homogeneous because they are created by the same geological process, and probably contain approximately the same rock types. Hence, at this scale it sounds reasonable to speak of an REV. If we move to the high end of the length-scale axis, we start to group more and more layers into families with different sedimentary structures, and REVs for porosity will probably not exist.

The discussion gives grounds to claim that reservoir rock structures contain scales where REVs may exist. From a general point of view, however, the existence of REVs in porous media is highly disputable. A faulted reservoir, for instance, can have faults distributed continuously both in length and aperture throughout the reservoir, and will typically have no REVs. Moreover, no two reservoirs are identical, so it is difficult to capitalize from

https://doi.org/10.1017/9781108591416.004 Published online by Cambridge University Press

previous experience. Indeed, porous formations in reservoirs may vary greatly, also in terms of scales. Nevertheless, the concept of REVs can serve as a guideline when deciding what scales to model.

2.3.3 Microscopic Models: The Pore Scale

Pore-scale models, as illustrated on the left-hand side of Figure 2.7, may be about the size of a sugar cube and are based on measurements from core plugs obtained from well trajectories during drilling. These rock samples are necessarily confined (in dimension) by the radius of the well, although they lengthwise are only confined by the length of the well. Three such rock samples are shown in Figure 2.9. The main methods for obtaining pore-scale models from a rock sample are by studying thin slices using an electron microscope with micrometer resolution or by CT scans. In the following, we will give a simplified overview of flow modeling on this scale.

At the pore scale, the porous medium is either represented by a volumetric grid or by a graph (see e.g., [242]). A graph is a pair (V, E), where V is a set whose elements are called vertices (or nodes), and E is a subset of $V \times V$ whose elements are called edges. The vertices are taken to represent pores, and the edges represent pore throats (i.e., connections between pores). The flow process, in which one fluid invades the void space filled by another fluid, is generally described as an invasion–percolation process dominated by capillary forces, in which a fluid phase can invade a pore only if a neighboring pore is already invaded. Another approach to multiphase modeling is through the use of the lattice Boltzmann method, which represents the fluids as a set of particles that propagate and collide according to a set of rules defined for interactions between particles of the same fluid phase, between particles of different fluid phases, and between the fluids and the walls of the void space. A further presentation of pore-scale modeling is beyond our scope here, but the interested reader is encouraged to consult, e.g., [242, 44] and references therein.

From an analytical point of view, pore-scale modeling is very important as it represents flow at the fundamental scale (or more loosely, where the flow really takes place), and

Figure 2.9 Three core plugs with a diameter of 3.81 cm and a height of 5 cm.

https://doi.org/10.1017/9781108591416.004 Published online by Cambridge University Press

hence provides the proper framework for understanding the fundamentals of porous media flow. From a practical point of view, pore-scale modeling has a huge potential. Modeling flow at all other scales can be seen as averaging of flow at the pore scale, and properties describing the flow at larger scales are usually a mixture of pore-scale properties. At larger scales, the complexity of flow modeling is often overwhelming, with large uncertainties in determining flow parameters. Hence being able to single out and estimate the various factors determining flow parameters is invaluable, and pore-scale models can be instrumental in this respect. However, to extrapolate properties from the pore scale to an entire reservoir is very challenging, even if the entire pore space of the reservoir was known. In real life you will of course not be anywhere close to knowing the entire pore space of a reservoir.

2.3.4 Mesoscopic Models

Models based on flow experiments on core plugs are by far the most common mesoscopic models. The main equations describing flow are continuity of fluid phases and Darcy's law, which states that flow rate is proportional to pressure drop. The purpose of core-plug experiments is to determine capillary pressure curves and the proportionality constant in Darcy's law that measures the ability to transmit fluids; see (1.2) in Section 1.4. To this end, the sides of the core are insulated and flow is driven through the core. By measuring flow rate versus pressure drop, one can estimate the proportionality constant for both single-phase and multiphase flows.

In conventional reservoir modeling, the effective properties from core-scale flow experiments are extrapolated to the macroscopic geological model, or directly to the simulation model. Cores should therefore ideally be representative for the heterogeneous structures in a typical grid block of the geological model, but flow experiments are usually performed on relatively homogeneous cores that rarely exceed one meter in length. Flow at the core scale is also more influenced by capillary forces than flow on a reservoir scale.

As a supplement to core-flooding experiments, it has in recent years become popular to build 3D grid models to represent small-scale geological details like the bedding structure and lithology (composition and texture). One example of such a model is shown in Figure 2.7. Effective flow properties for the 3D model can now be estimated in the same way as for core plugs by replacing the flow experiment by flow simulations using rock properties that are, e.g., based on the input from microscopic models. This way, one can incorporate fine-scale geological details from lamina into the macroscopic reservoir models. However, the process of extrapolating information from cores to build a geological model is largely underdetermined and must generally be supplied with geological data from other sources.

2.4 Modeling Rock Properties

Describing the flow through a porous rock structure is largely a question of the scale of interest. The size of the rock bodies forming a typical petroleum reservoir will be from 10 to 100 meters in the vertical direction and several hundred meters or a few kilometers

https://doi.org/10.1017/9781108591416.004 Published online by Cambridge University Press

in the lateral direction. On this scale, it is clearly impossible to describe the storage and transport in individual pores and pore channels, as discussed in Section 2.3.3, or through individual laminae, as in Section 2.3.4. To obtain a description of the reservoir geology, one builds models that attempt to reproduce the true geological heterogeneity in the reservoir rock at the macroscopic scale by introducing macroscopic petrophysical properties based on a continuum hypothesis and volume averaging over a sufficiently large REV. These petrophysical properties are engineering quantities that are used as input to flow simulators, and are not true geological or geophysical properties of the underlying media.

A geological model is a conceptual, three-dimensional representation of a reservoir, whose main purpose is to give a spatial representation of the ability to store and transmit fluids, besides giving location and geometry of the reservoir. The rock body itself is modeled in terms of a volumetric grid, in which the layered structure of sedimentary beds and the geometry of faults and large-scale fractures in the reservoir are represented by the geometry and topology of the grid cells. Cell sizes in geocellular models can vary a lot, but typical sizes are in the range of 0.1–1 m in the vertical direction and 10–50 m in the horizontal direction. The petrophysical properties of the rock are represented as constant values inside each grid cell (porosity and permeability) or as values attached to cell faces (fault multipliers, fracture apertures, etc.). In the following sections, we will describe the main rock properties in more detail. More details about the grid modeling will follow in Chapter 3.

2.4.1 Porosity

The porosity ϕ of a porous medium is defined as the fraction of the bulk volume that represents void space, which means that $0 \leq \phi < 1$. Likewise, $1 - \phi$ is the fraction occupied by solid material (rock matrix). The void space generally consists of two parts: interconnected pore space available to fluid flow, and disconnected pores (dead ends) that are unavailable to flow. Only the first part is interesting for flow simulation, and porosity is therefore usually a shorthand for the "effective porosity" that measures the fraction of connected void space to bulk volume.

For a completely rigid medium, porosity is a static, dimensionless quantity that can be measured in the absence of flow. Porosity is mainly determined by the pore and grain-size distribution. Rocks with nonuniform grain size usually have smaller porosity than rocks with a uniform grain size, because smaller grains tend to fill pores formed by larger grains. For a bed of solid spheres of uniform diameter, the porosity depends on the packing, varying between 0.2595 for a rhomboidal packing to 0.4764 for cubic packing. When sediments are first deposited in water, they usually have a porosity of approximately 0.5, but as they are buried, the water is gradually squeezed out and the void space between the mineral particles decreases as the sediments are consolidated into rocks. For sandstone and limestone, ϕ is in the range 0.05–0.5, although values outside this range may be infrequently observed. Sandstone porosity is usually determined by the sedimentological process by

https://doi.org/10.1017/9781108591416.004 Published online by Cambridge University Press

which the rock was deposited, whereas carbonate porosity is mainly a result of changes taking place after deposition. Increase compaction (and cementation) causes porosity to decrease with depth in sedimentary rocks. The porosity can also be reduced by minerals that are deposited as water moves through pore spaces. For sandstone, the loss in porosity is small, whereas shales loose their porosity very quickly. Shales are therefore unlikely to be good reservoir rocks in the conventional sense, and will instead act like caprocks having porosities that are orders of magnitude lower than those found in good sandstone and carbonates.

For non rigid rocks, the porosity is usually modeled as a pressure-dependent parameter. That is, one says that the rock is *compressible*, having a rock compressibility defined by

$$c_r = \frac{1}{\phi}\frac{d\phi}{dp} = \frac{d\ln(\phi)}{dp}, \tag{2.1}$$

where p is the overall reservoir pressure. Compressibility can be significant in some cases, e.g., as evidenced by the subsidence observed in the Ekofisk area in the North Sea. For a rock with constant compressibility, (2.1) can be integrated to give

$$\phi(p) = \phi_0 e^{c_r(p-p_0)}, \tag{2.2}$$

and for simplified models, it is common to use a linearization so that:

$$\phi = \phi_0\big[1 + c_r(p - p_0)\big]. \tag{2.3}$$

Because the dimension of the pores is very small compared to any interesting scale for reservoir simulation, one normally assumes that porosity is a piecewise continuous spatial function. However, ongoing research aims to understand better the relation between flow models on pore scale and on reservoir scale.

2.4.2 Permeability

Permeability is a basic flow property of a porous medium and measures its ability to transmit a single fluid when the void space is completely filled with this fluid. This means that permeability, unlike porosity, is a parameter that cannot be defined apart from fluid flow. The precise definition of the (absolute, specific, or intrinsic) permeability K is as the proportionality factor between the flow rate and an applied pressure or potential gradient $\nabla\Phi$,

$$\vec{v} = -\frac{K}{\mu}\nabla\Phi. \tag{2.4}$$

This relationship is called Darcy's law after the french hydrologist Henry Darcy, who first observed it in 1856 while studying flow of water through beds of sand [77]. In (2.4), μ is the fluid viscosity and $\vec{v}$ is the *superficial velocity*, i.e., the flow rate divided by the cross-sectional area perpendicular to the flow. This should not be confused with the interstitial velocity $\vec{u} = \phi^{-1}\vec{v}$, i.e., the rate at which an actual fluid particle moves through the medium. We will come back to a more detailed discussion of Darcy's law in Section 4.1.

https://doi.org/10.1017/9781108591416.004 Published online by Cambridge University Press

The SI-unit for permeability is m^2, which reflects the fact that permeability is determined entirely by the geometric characteristics of the pores. However, it is more common to use the unit "darcy" (D). The precise definition of 1 D $\approx 0.987 \cdot 10^{-12}$ m^2 involves transmission of a 1 cP fluid through a homogeneous rock at a speed of 1 cm/s due to a pressure gradient of 1 atm/cm. Translated to reservoir conditions, 1 D is a relatively high permeability and it is therefore customary to specify permeabilities in millidarcys (md or mD). Rock formations like sandstones tend to have many large or well-connected pores and therefore transmit fluids readily. They are therefore described as permeable. Other formations, like shales, may have smaller, fewer, or less interconnected pores and are hence described as impermeable. Conventional reservoirs have permeabilities ranging from 0.1 mD to 20 D for liquid flow, and down to 10 mD for gases. In recent years, however, there has been an increasing interest in unconventional resources, that is, gas and oil locked in extraordinarily impermeable and hard rocks, with permeability values ranging from 0.1 mD and down to 1 μD or lower. *"Tight"* reservoirs are defined as those having permeability less than 0.1 mD. Compared with conventional resources, the potential volumes of tight gas, shale gas, and shale oil are enormous, but cannot be easily produced at economic rates unless stimulated, e.g., using a pressurized fluid to break up the rock to create new flow paths (hydraulic fracturing). This book focuses exclusively on simulation of conventional resources.

In (2.4), we tacitly assumed that K is a scalar quantity. However, permeability will generally be a full tensor,

$$\mathbf{K} = \begin{bmatrix} K_{xx} & K_{xy} & K_{xz} \\ K_{yx} & K_{yy} & K_{yz} \\ K_{zx} & K_{zy} & K_{zz} \end{bmatrix}. \tag{2.5}$$

Here, the diagonal terms $\{K_{xx}, K_{yy}, K_{zz}\}$ represent how the flow rate in one axial direction depends on the pressure drop in the same direction. The off-diagonal terms $\{K_{xy}, K_{xz}, K_{yx}, K_{yz}, K_{zx}, K_{zy}\}$ account for dependence between flow rate in one axial direction and the pressure drop in perpendicular directions. A full tensor is needed to model local flow in directions at an angle to the coordinate axes. Let us for instance consider a layered system, for which the dominant direction of flow will generally be along the layers. However, if the layers form an angle to the coordinate axes, a pressure drop in one coordinate direction will produce flow at an angle to this direction. This type of flow can only be modeled correctly with a permeability tensor with nonzero off-diagonal terms. If the permeability can be represented by a scalar function $K(\vec{x})$, we say that the permeability is *isotropic* as opposed to the *anisotropic* case where we need a full tensor $\mathbf{K}(\vec{x})$. To model a physical system, the anisotropic permeability tensor must be symmetric because of the Onsager principle of reciprocal relations and positive definite because the flow component parallel to the pressure drop should be in the same direction as the pressure drop. As a result, a full-tensor permeability $\mathbf{K}$ may be diagonalized by a change of basis.

https://doi.org/10.1017/9781108591416.004 Published online by Cambridge University Press

Since the porous medium is formed by deposition of sediments over thousands of years, there is often a significant difference between permeability in the vertical and lateral directions, but no difference between the permeabilities in the two lateral directions. The permeability is obviously also a function of porosity. Assuming a laminar flow (low Reynolds numbers) in a set of capillary tubes, one can derive the Carman–Kozeny relation,

$$K = \frac{1}{8\tau A_v^2} \frac{\phi^3}{(1-\phi)^2}, \tag{2.6}$$

which relates permeability to porosity ϕ, but also shows that the permeability depends on local rock texture described by tortuosity τ and specific surface area A_v. The *tortuosity* is defined as the squared ratio of the mean arc–chord length of flow paths, i.e., the ratio between the length of a flow path and the distance between its ends. The *specific surface area* is an intrinsic and characteristic property of any porous medium that measures the internal surface of the medium per unit volume. Clay minerals, for instance, have large specific surface areas and hence low permeability. The quantities τ and A_v can be calculated for simple geometries, e.g., for engineered beds of particles and fibers, but are rarely measured for reservoir rocks. Moreover, the relationship in (2.6) is highly idealized and only gives satisfactory results for media consisting of grains that are approximately spherical and have a narrow size distribution. For consolidated media and cases in which rock particles are far from spherical and have a broad size distribution, the simple Carman–Kozeny equation does not apply. Instead, permeability is typically obtained through macroscopic flow measurements.

Permeability is generally heterogeneous in space because of different sorting of particles, degree of cementation (filling of clay), and transitions between different rock formations. Indeed, the permeability may vary rapidly over several orders of magnitude; local variations in the range 1 mD to 10 D are not unusual in field and sector models. The heterogeneous structure of a porous rock formation is a result of the deposition and geological history and will therefore vary strongly from one formation to another, as we will see in a few of the examples in Section 2.5.

Production of fluids may also change the permeability. When temperature and pressure are changed, microfractures may open and significantly change the permeability. Furthermore, since the definition of permeability involves a certain fluid, different fluids will experience different permeability in the same rock sample. Such rock–fluid interactions are discussed in Chapter 8.

2.4.3 Other Parameters

Not all the bulk volume in a reservoir zone consist of reservoir rocks. To account for the fact that some portion of a cell may contain impermeable shale, it is common to introduce the so-called *net-to-gross* (N/G) property, which is a number in the range 0–1 that represents the fraction of reservoir rock in a cell. To get the effective porosity of a given cell, one must multiply the porosity and N/G value of the cell. (The N/G values also act as multipliers

https://doi.org/10.1017/9781108591416.004 Published online by Cambridge University Press

for lateral transmissibilities, which we will come back to later in the book.) A zero value means that the corresponding cell only contains shale (either because the porosity, the N/G value, or both are zero), and such cells are by convention typically not included in the active model.

Faults can either act as conduits for fluid flow in subsurface reservoirs or create flow barriers and introduce compartmentalization that severely affects fluid distribution and/or reduces recovery. On a reservoir scale, faults are generally volumetric objects that can be described in terms of displacement and petrophysical alteration of the surrounding host rock. However, lack of geological resolution in simulation models means that fault zones are commonly modeled as surfaces that explicitly approximate the faults' geometrical properties. To model the hydraulic properties of faults, one introduces so-called *multipliers* that alter the ability to transmit fluid between two neighboring cells. Multipliers can also model other types of subscale features that affect the communication between grid blocks, e.g., thin mud layers resulting from a flooding event, which may partially cover the sand bodies and reduce vertical communication. It is also common to (ab)use multipliers to increase or decrease the flow in certain parts of the model to calibrate simulated reservoir responses to historic data (production curves from wells, etc.). More details about multipliers will be given later in the book.

2.5 Property Modeling in MRST

All flow and transport solvers in MRST assume that rock parameters are represented as fields in a structure array (struct), which by convention is called `rock`. You do not need to follow this convention, but `rock` must contain two subfields called `poro` and `perm`. The porosity field `rock.poro` is a vector with one value for each active cell in the associated grid model. The permeability field `rock.perm` can either contain a single column for an isotropic permeability, two or three columns for a diagonal permeability (in 2D and 3D, respectively), or six columns for a symmetric, full-tensor permeability. In the latter case, cell number i has the permeability tensor

$$\mathbf{K}_i = \begin{bmatrix} K_1(i) & K_2(i) \\ K_2(i) & K_3(i) \end{bmatrix}, \qquad \mathbf{K}_i = \begin{bmatrix} K_1(i) & K_2(i) & K_3(i) \\ K_2(i) & K_4(i) & K_5(i) \\ K_3(i) & K_5(i) & K_6(i) \end{bmatrix},$$

where $K_j(i)$ is the entry in column j and row i of `rock.perm`. Full-tensor, nonsymmetric permeabilities are currently not supported. In addition to porosity and permeability, MRST supports a field called `ntg` representing the net-to-gross ratio, which either consists of a scalar or a single column with one value per active cell.

The rest of this section demonstrate how to generate and specify rock parameters in MRST and briefly outlines a few realistic models. The discussion will also expose you to a standard visualization capabilities in MRST. Scripts containing the code lines necessary to reproduce all figures can be found in the `rock` subdirectory of the `book` module.

https://doi.org/10.1017/9781108591416.004 Published online by Cambridge University Press

2.5.1 Homogeneous Models

Homogeneous models are very simple to specify. To exemplify, consider a square 10×10 grid model with a uniform porosity of 0.2 and isotropic permeability equal 200 mD:

```
G = cartGrid([10 10]);
rock = makeRock(G, 200*milli*darcy, 0.2);
```

Because MRST works in SI units, it is important to convert from the field unit "darcy" to the SI unit "meters^2." Here, we did this by multiplying with `milli` and `darcy`, which are two functions that return the corresponding conversion factors. Alternatively, we could have used the conversion function `convertFrom(200, milli*darcy)`. Homogeneous, anisotropic permeability can be specified in the same way:

```
rock = makeRock(G, [100 100 10].*milli*darcy, 0.2);
```

2.5.2 Random and Lognormal Models

Given the difficulty of measuring rock properties, it is common to use geostatistical methods to make realizations of porosity and permeability. MRST contains two *very* simplified methods for generating geostatistical realizations. For more realistic geostatistics, you should use GSLIB [82] or a commercial geomodeling software.

In our first example, we will generate the porosity ϕ as a Gaussian field. To get a crude approximation to the permeability–porosity relationship, we assume that our medium is made up of uniform spherical grains of diameter $d_p = 10\,\mu\text{m}$, for which the specific surface area is $A_v = 6/d_p$. Using the Carman–Kozeny relation (2.6), we can then calculate the isotropic permeability K from

$$K = \frac{1}{72\tau}\frac{\phi^3 d_p^2}{(1-\phi)^2},$$

where we further assume that $\tau = 0.81$. As a simple approximation to a Gaussian porosity field, we generate a field of independent normally distributed variables using MATLAB's built-in `rand` function, convolve it with a Gaussian kernel, and scale the result to the interval $[0.2, 0.4]$:

```
G = cartGrid([50 20]);
p = gaussianField(G.cartDims, [0.2 0.4], [11 3], 2.5);
K = p.^3.*(1e-5)^2./(0.81*72*(1-p).^2);
rock = makeRock(G, K(:), p(:));
```

The left plot of Figure 2.10 shows the resulting porosity field, whereas the right plot shows the permeability obtained for a 3D realization with $50 \times 20 \times 10$ cells generated in the same way.

https://doi.org/10.1017/9781108591416.004 Published online by Cambridge University Press

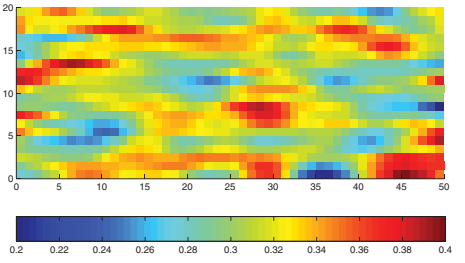


```
plotCellData(G,rock.poro,'EdgeColor','none');
colorbar('horiz'); axis equal tight;
```

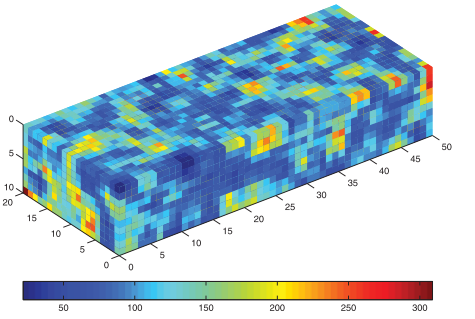


```
plotCellData(G,convertTo(rock.perm,milli*darcy));
colorbar('horiz'); axis equal tight; view(3);
```

Figure 2.10 The left plot shows a 50×20 porosity field generated as a Gaussian field with a larger filter size in x-direction than in the y-direction. The right plot shows the permeability field computed from the Carman–Kozeny relation for a similar $50 \times 20 \times 10$ porosity realization computed with filter size $[3, 3, 3]$.

In the second example, we use the same methodology to generate layered realizations, defined so that the permeability is lognormally distributed in each geological layer and independent of the other layers. Each layer can be represented by several grid cells in the vertical direction. Rather than using a simple Cartesian grid, we generate a stratigraphic grid with wavy geological faces and a single fault. Chapter 3 describes this type of industry-standard grids in more detail.

```
G = processGRDECL(simpleGrdecl([50 30 10], 0.12));
K = logNormLayers(G.cartDims, [100 400 50 350], 'indices', [1 2 5 7 11]);
```

Here, we have specified four geological layers of different thickness. From top to bottom, which is the default numbering in stratigraphic grids, the first layer is one cell thick and has a mean permeability value of 100 mD, the second layer is three cells thick and has mean permeability of 400 mD, the third layer is two cells thick and has mean value 50 mD, and the fourth layer is four cells thick and has mean value 350 mD. To specify this, we use an indirection map; that is, if `Km` is the n-vector of mean permeabilities and `L` is the $(n + 1)$-vector of indices, the value `Km(i)` is assigned to vertical layers number `L(i)` to `L(i+1)-1`. Figure 2.11 shows the resulting permeability field.

2.5.3 The 10th SPE Comparative Solution Project: Model 2

The Society of Petroleum Engineers (SPE) has developed a series of benchmarks for comparing computational methods and simulators. The first nine benchmarks focus on black-oil, compositional, dual-porosity, thermal, and miscible simulations, as well as horizontal wells and gridding techniques. The 10th SPE Comparative Solution Project [71]

https://doi.org/10.1017/9781108591416.004 Published online by Cambridge University Press

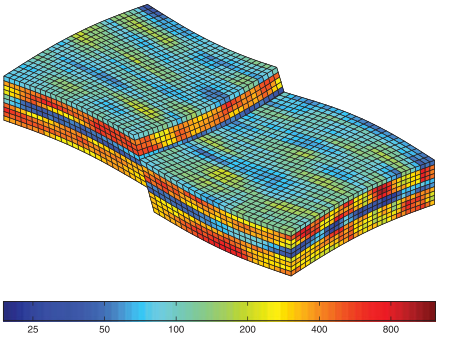


```
plotCellData(G,log10(K),'EdgeColor','k');
view(45,30);
axis tight off,
set(gca,'DataAspect',[0.5 1 1])
h=colorbar('horiz');
ticks=25*2.^[0:5];
set(h,'XTick', log10(ticks), ...
    'XTickLabel', ticks);
```

Figure 2.11 A stratigraphic grid with a single fault and four geological layers, each with a lognormal permeability distribution.

was posed as a benchmark for upscaling methods, but the second data set of this benchmark has later become very popular as a general test case within the academic community. The data set is a 3D geostatistical realization from the Jurassic Upper Brent formations from the North Sea, which, e.g., contains the giant fields of Statfjord, Gullfaks, Oseberg, and Snorre. The main features of the model are the permeability and porosity fields given on a $60 \times 220 \times 85$ Cartesian grid, in which each cells is of size 20 ft $\times$ 10 ft $\times$ 2 ft. In this specific model, the top 35 cell layers having a total height of 70 ft represent the shallow-marine Tarbert formation, and the lower 50 layers having a height of 100 ft represent the fluvial Ness formation. The original geostatistical model was developed in the PUNQ project [111], and later the horizontal dimensions were scaled by a factor 1/3 to make it more heterogeneous. The model is structurally simple but is highly heterogeneous, and, for this reason, some describe it as a "simulator-killer." On the other hand, the fact that the flow is dictated by the strong heterogeneity means that streamline methods will be particularly efficient for this model [4].

The SPE 10 data set is used in a large number of publications and is publicly available from the SPE website (http://www.spe.org/web/csp/). MRST supplies a module called `spe10` that downloads, reorganizes, and stores the data set in `*.mat` files for later use. The module also contains routines that extract (subsets of) the petrophysical data and set up simulation models and appropriate data structures representing grids, petrophysics, and wells. Alternatively, the data set can be downloaded using `mrstDatasetGUI`. We start by loading the petrophysical data

```
% load SPE 10 data set
mrstModule add spe10;
rock = getSPE10rock(); p=rock.poro; K=rock.perm;
```

Because of the simple Cartesian grid topology, we can use standard MATLAB functionality to visualize the heterogeneity in the permeability and porosity (full details can be found in the script `rocks/showSPE10.m`):

https://doi.org/10.1017/9781108591416.004 Published online by Cambridge University Press

```
slice( reshape(p,60,220,85), [1 220], 60, [1 85]);
shading flat, axis equal off, set(gca,'zdir','reverse'), box on;
colorbar('horiz');

% show Kx
slice( reshape(log10(K(:,1)),60,220,85), [1 220], 60, [1 85]);
shading flat, axis equal off, set(gca,'zdir','reverse'), box on;
h=colorbar('horiz');
set(h,'XTickLabel',10.^[get(h,'XTick')]);
set(h,'YTick',mean(get(h,'YLim')),'YTickLabel','mD');
```

Figure 2.12 shows porosity and permeability; the permeability tensor is diagonal with equal permeability in the two horizontal coordinate directions. Both formations are characterized by large permeability variations, 8–12 orders of magnitude, but are qualitatively different. The Tarbert consists of sandstone, siltstone, and shales, and comes from a tidally influenced, transgressive, shallow-marine deposit; in other words, a deposit that has taken place close to the coastline; see Figure 2.1. The formation has good communication in the vertical and horizontal directions. The fluvial Ness formation has been deposited by rivers or running water in a delta-plain, continental environment (see Figures 2.1 and 2.2), leading to a spaghetti of well-sorted, high-permeable sandstone channels with good communication

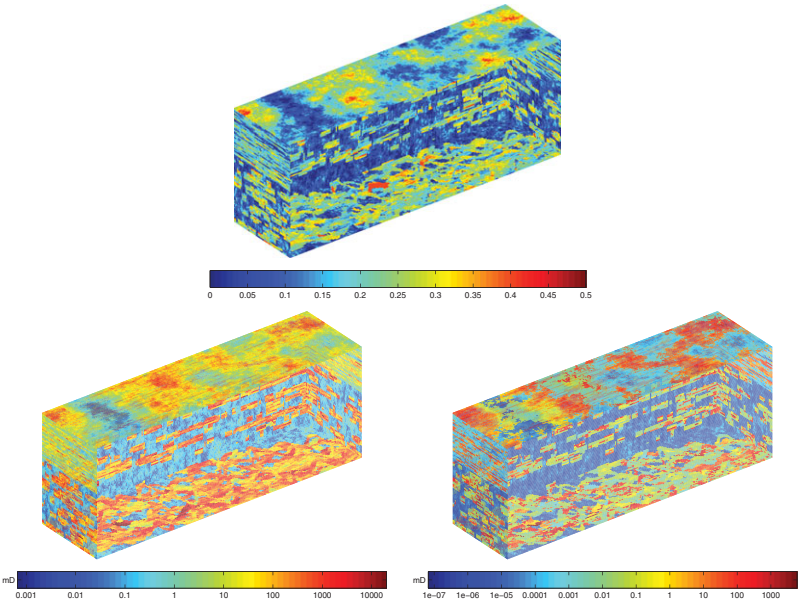

Figure 2.12 Rock properties for the SPE 10 model. The upper plot shows the porosity, the lower left the horizontal permeability, and the lower right the vertical permeability. (The permeabilities are shown using a logarithmic color scale.)

https://doi.org/10.1017/9781108591416.004 Published online by Cambridge University Press

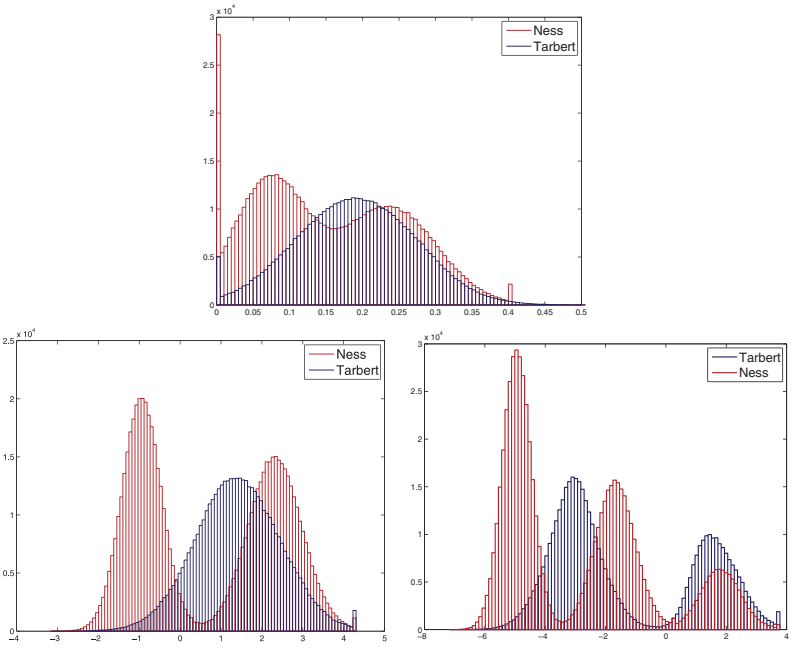

Figure 2.13 Histogram of rock properties for the SPE 10 model: ϕ (upper plot), $\log \mathbf{K}_x$ (lower left), and $\log \mathbf{K}_z$ (lower right) The Tarbert formation is shown in blue and the Ness formation in red.

(long correlation lengths) imposed on a low-permeable background of shales and coal, which gives low communication between different sand bodies. The porosity field has a large span of values, and approximately 2.5% of the cells have zero porosity and should be considered as being inactive.

Figure 2.13 shows histograms of the porosity and the logarithm of the horizontal and vertical permeabilities. The nonzero porosity values and the horizontal permeability of the Tarbert formation appear to follow a normal and lognormal distribution, respectively. The vertical permeability follows a bimodal distribution. For the Ness formation, the nonzero porosities and the horizontal permeability follow bi-modal normal and lognormal distributions, respectively, as is to be expected for a fluvial formation. The vertical permeability is trimodal. To five significant digits, the ratio of vertical to horizontal permeability has two unique values 10^{-4} and 0.3, which together with the K index can be used to distinguish the three different rock types (facies) in the model: sheet sand and mudstone in the Tarbert formation, and channel sand and mudstone in Upper Ness.

2.5.4 The Johansen Formation

The Johansen formation is located in the deeper part of the Sognefjord delta, 40–90 km offshore Mongstad on the west coast of Norway. Some years ago, a gas power plant with

https://doi.org/10.1017/9781108591416.004 Published online by Cambridge University Press

carbon capture and storage was planned at Mongstad, and the water-bearing Johansen formation was a possible candidate for storing the captured CO_2. The Johansen formation is part of the Dunlin group, and is interpreted as a large sandstone delta 2,200–3,100 m below sea level, which is limited above by the Dunlin shale and below by the Amundsen shale. The average thickness of the formation is roughly 100 m, and the aquifer extends laterally up to 100 km in the north–south direction and 60 km in the east–west direction. The aquifer has good sand quality and lies at a depth where CO_2 would undoubtedly be in supercritical phase, and would thus be ideal for carbon storage. With average porosities of approximately 25%, this implies that the theoretical storage capacity of the Johansen formation is more than one gigatonne of CO_2 [97]. The Troll field, one of the largest gas fields in the North Sea, is located some 500 m above the northwestern parts of the Johansen formation.

A previous research project generated several models of the Johansen formation using so-called corner-point grids. We will discuss this format in more detail in Section 3.3.1. For now, it is sufficient to note that corner-point grids consist of (distorted) hexahedral cells organized according to an underlying Cartesian topology. Altogether, there are five models: one full-field model ($149 \times 189 \times 16$ grid), three homogeneous sector models ($100 \times 100 \times n$ for $n = 11, 16, 21$), and one heterogeneous sector model ($100 \times 100 \times 11$). All models are publicly available on the MRST website and can, for instance, be downloaded to MRST using the `mrstDatasetGUI` function. Herein, we consider the heterogeneous sector model. You can find all statements used in the following analysis in the script `rocks/showJohansenNPD.m`.

We start by reading the grid geometry from an industry-standard input format, which we discuss in more detail in the next section, and then construct a corresponding MRST grid structure. The rock properties are given as plain ASCII files that each contains 110,000 values. Some of these values correspond to logical cell indices that are not part of the actual simulation model and can be discarded if we use the indirection map `G.cells.indexMap` to extract the correct subset:

```
G = processGRDECL(readGRDECL('NPD5.grdecl'));
p = load('NPD5_Porosity.txt')'; p = p(G.cells.indexMap);
K = load('NPD5_Permeability.txt')'; K=K(G.cells.indexMap);
```

In the model, the Johansen formation is represented by five layers of cells, whereas the low-permeable Dunlin shale above and the Amundsen shale below are represented by five and one cell layers. The Johansen formation consists of approximately 80% sandstone and 20% claystone, whereas the Amundsen formation consists of siltstones and shales; see [97] for more details. In the left plot of Figure 2.14, the Johansen sand is clearly distinguished as a wedge shape that is pinched out in the front part of the model and splits the shales laterally in two at the back. The right plot shows the good reservoir rocks distinguished as cells with a porosity value larger than 0.1. The permeability tensor is assumed to be diagonal, with the vertical permeability equaling one-tenth of the horizontal permeability. Hence, only the x-component $\mathbf{K}_x$ is given in the data file. Figure 2.15 shows three different plots of the

https://doi.org/10.1017/9781108591416.004 Published online by Cambridge University Press

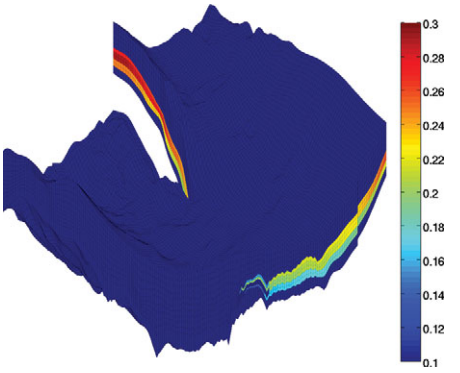


```
args = {'EdgeAlpha'; 0.1; 'EdgeColor'; 'k'};
plotCellData(G, p, args{:}); view(-45,15),
axis tight off, zoom(1.15),
caxis([0.1 0.3]), colorbar;
```

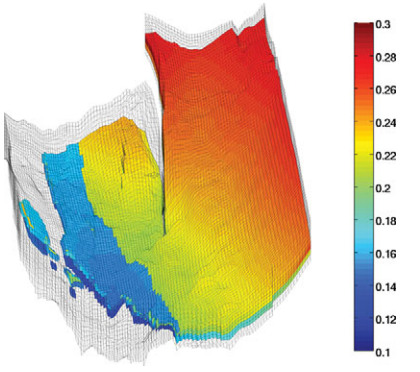


```
plotGrid(G,'FaceColor','none', args{:});
plotCellData(G, p, find(p>0.1), args{:})
view(-15,40); axis tight off, zoom(1.15),
caxis([0.1 0.3]), colorbar;
```

Figure 2.14 Porosity for the Johansen data set "NPD5." The left plot shows porosity for the whole model, whereas in the right plot we have masked the low-porosity cells in the Amundsen and Dunlin formations.

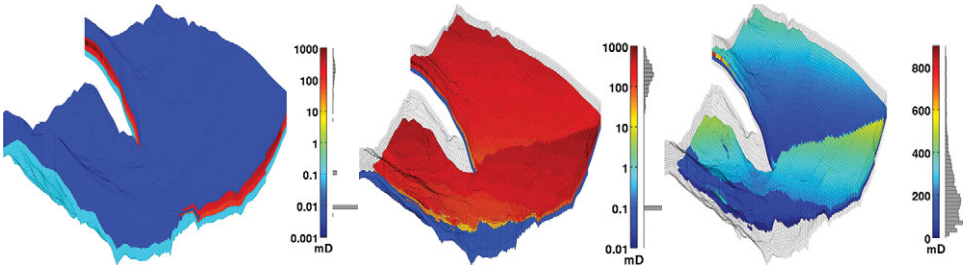

Figure 2.15 Permeability for the Johansen data set "NPD5." The left plot shows permeability for the whole model, the middle plot shows the Johansen sand and Amundsen shale, whereas the right plot only shows permeability of the Johansen sand.

permeability. The first plot presents the whole permeability field with a logarithmic color scale. In the second plot, we have filtered out the Dunlin shale above Johansen but not the Amundsen shale below. The third plot depicts the permeability in the Johansen formation using a linear color scale, which clearly shows the depth trend that was used to model the heterogeneity.

2.5.5 SAIGUP: Shallow-Marine Reservoirs

Most commercial simulators use a combination of an *input language* and a set of data files to describe and set up a simulation model of a reservoir. In this book, we only discuss the

https://doi.org/10.1017/9781108591416.004 Published online by Cambridge University Press

ECLIPSE input format, which has emerged as an industry standard for describing static and dynamic properties of a reservoir system, from the reservoir rock, via production and injection wells and up to connected top-side facilities. ECLIPSE input decks use keywords to signify and separate the different data elements that comprise a full model. These keywords define a detailed language you can use to specify how the data elements should be put together and modify each other to form a full spatio-temporal model of a reservoir. In the most general form, an ECLIPSE input deck consists of eight sections of keywords that must come in a prescribed order. However, some of the sections are optional and may not always be present. The order of the keywords within each section is arbitrary, except in the section that defines wells and gives operating schedule, etc. Altogether, the ECLIPSE format consists of thousands of keywords, and describing them all is far beyond the scope of this book. Other simulators use a somewhat different syntax, but the principles of the overall input description is often similar.

In the following, we briefly outline some of the most common keywords from the GRID section that describes the reservoir geometry and petrophysical properties. To provide you with a basic understanding of the required input for simulating real-life reservoir models, we focus on the model ingredients and not on the specific syntax. For brevity, we also do not go through all MATLAB and MRST statements used to visualize the different data elements. All the necessary details can be found in the script `rocks/showSAIGUP.m`.

As our example of a realistic petroleum reservoir, we consider a model from the SAIGUP study [203], whose purpose was to conduct a sensitivity analysis of how geological uncertainties impacts production forecasting in clastic reservoirs. To this end, the study generated a large suite of geostatistical realizations and structural models to represent a wide span of shallow-marine sedimentological reservoirs. The SAIGUP study focused on shoreface reservoirs in which the deposition of sediments is caused by variation in sea level, so that facies form belts in a systematic pattern (river deposits create curved facies belts, wave deposits create parallel belts, etc.). Sediments are in general deposited when the sea level is increasing. No sediments are deposited during decreasing sea levels; instead, the receding sea may affect the appearing shoreline and cause the creation of a barrier. All models are synthetic, but contain representative examples of the complexities seen in real-life reservoirs.

One of the many SAIGUP realizations is publicly available from the MRST website and comes in the form of a GZip-compressed TAR file (`SAIGUP.tar.gz`) that contains the structural model as well as petrophysical parameters. You can download the data set using the `mrstDatasetGUI` function. Here, however, we unpack the data set manually for completeness of presentation. Assuming that we have already downloaded the archive file `SAIGUP.tar.gz` with the model realization, we extract the data files and place them in a standardized path relative to the root directory of MRST:

```
untar('SAIGUP.tar.gz', fullfile(ROOTDIR, 'examples', 'data', 'SAIGUP'))
```

https://doi.org/10.1017/9781108591416.004 Published online by Cambridge University Press

This will create a new directory containing seventeen data files that comprise the structural model, various petrophysical parameters, etc.:

```
028_A11.EDITNNC      028.MULTX  028.PERMX  028.SATNUM       SAIGUP.GRDECL
028_A11.EDITNNC.001  028.MULTY  028.PERMY  SAIGUP_A1.ZCORN
028_A11.TRANX        028.MULTZ  028.PERMZ  SAIGUP.ACTNUM
028_A11.TRANY        028.NTG    028.PORO   SAIGUP.COORD
```

The main file is `SAIGUP.GRDECL`, which lists the sequence of keywords that specifies how the data elements found in the other files should be put together to make a complete model of the reservoir rock. The remaining files represent different keywords: the grid geometry is given in files `SAIGUP_A1.ZCORN` and `SAIGUP.COORD`, the porosity in `028.PORO`, the permeability tensor in the three `028.PERM*` files, net-to-gross properties in `028.NTG`, the list of active cells in `SAIGUP.ACTNUM`, transmissibility multipliers that modify the flow connections between different cells are given in `028.MULT*`, etc. For now, we rely entirely on MRST's routines for reading ECLIPSE input files; more details about corner-point grids and the ECLIPSE input format will follow later in the book, starting in Chapter 3.

The `SAIGUP.GRDECL` file contains seven of the eight possible sections of a full input deck. The `deckformat` module in MRST contains a comprehensive set of input routines that enable you to read the most important keywords and options supported in these sections. For the SAIGUP model, it is mainly the sections describing static reservoir properties that contain complete and useful information, and we will therefore use the much simpler function `readGRDECL` from MRST core to read and interpret the GRID section of the input deck:

```
grdecl = readGRDECL(fullfile(ROOTDIR, 'examples', ...
   'data', 'SAIGUP','SAIGUP.GRDECL'));
```

This statement parses the input file and stores the content of all keywords it recognizes in the structure `grdecl`:

```
grdecl =
    cartDims: [40 120 20]
       COORD: [29766x1 double]
       ZCORN: [768000x1 double]
      ACTNUM: [96000x1 int32]
       PERMX: [96000x1 double]
       PERMY: [96000x1 double]
       PERMZ: [96000x1 double]
       MULTX: [96000x1 double]
       MULTY: [96000x1 double]
       MULTZ: [96000x1 double]
        PORO: [96000x1 double]
         NTG: [96000x1 double]
      SATNUM: [96000x1 double]
```

The first four data fields describe the grid, and we will come back to these in Section 3.3.1. In the following, we discuss the next eight data fields, which contain the petrophysical parameters. We also look briefly at the last data field, which delineates the reservoir into different (user-defined) rock types that can be used to associate different rock-fluid properties.

https://doi.org/10.1017/9781108591416.004 Published online by Cambridge University Press

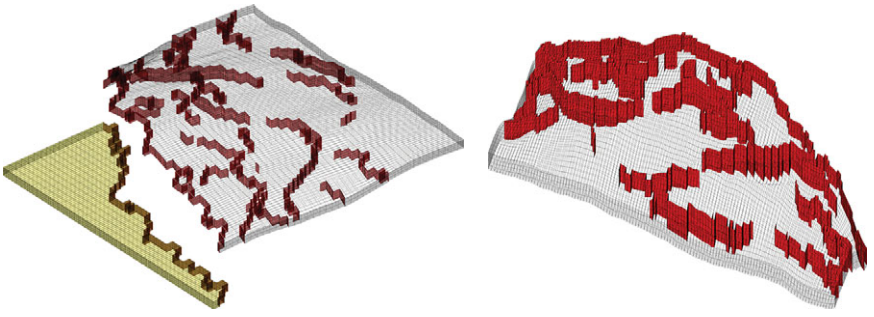

Figure 2.16 The structural SAIGUP model. The left plot shows the full model with faults marked in red and inactive cells marked in yellow, whereas the right plot shows only the active parts of the model seen from the opposite direction.

Recall that MRST uses strict SI conventions in all of its internal calculations. The SAIGUP model follows the ECLIPSE "METRIC" conventions (permeabilities in mD and so on). We thus use functions `getUnitSystem` and `convertInputUnits` to convert the input data to MRST's internal unit conventions.

```
usys   = getUnitSystem('METRIC');
grdecl = convertInputUnits(grdecl, usys);
```

Having converted the units properly, we generate a space-filling grid and extract the petrophysical properties:

```
G = processGRDECL(grdecl);
G = computeGeometry(G);
rock   = grdecl2Rock(grdecl, G.cells.indexMap);
```

The first statement takes the description of the grid geometry and constructs an unstructured MRST grid represented with the data structure outlined in Section 3.4. The second statement computes a few geometric primitives like cell volumes, centroids, etc., as discussed on page 93. The third statement constructs a rock object containing porosity, permeability, and net-to-gross.

For completeness, we first show a bit more details of the structural model in Figure 2.16. The left plot shows the whole $40 \times 120 \times 20$ grid model,[1] where we in particular should note the disconnected cells marked in yellow that are not part of the active model. The large fault throw that disconnects the two parts is most likely a modeling artifact introduced to clearly distinguish the active and inactive parts of the model. A shoreface reservoir is bounded by faults and geological horizons, but faults also appear inside the reservoir, as the right plot in Figure 2.16 shows. Faults and barriers will typically have a pronounced effect on the

[1] To not confuse the reader, I emphasize that only the active part of the model is read with the processGRDECL routine. How to also include the inactive part, will be explained in more detail in Chapter 3.

https://doi.org/10.1017/9781108591416.004 Published online by Cambridge University Press

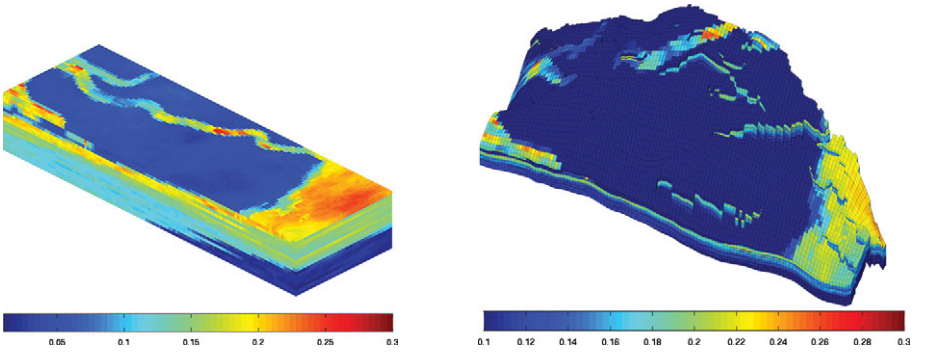


```
p = reshape(grdecl.PORO, G.cartDims);
slice(p, 1, 1, 1); view(-135,30), shading flat,
axis equal off,
set(gca,'ydir','reverse','zdir','reverse')
colorbar('horiz'); caxis([0.01 0.3]);
```

```
args = {'EdgeAlpha'; 0.1; 'EdgeColor'; 'k'};
plotCellData(G,rock.poro, args{:});
axis tight off; set(gca,'DataAspect',[1 1 0.1]);
view(-65,55); zoom(1.4); camdolly(0,-0.2,0)
colorbar('horiz'); caxis([0.1 0.3])
```

Figure 2.17 Porosity for the SAIGUP model. The left plot shows porosity as generated by geostatistics in logical ijk space. The right plot shows the porosity mapped to the structural model shown in Figure 2.16.

flow pattern, and having an accurate representation is important to produce reliable flow predictions.

The petrophysical parameters for the model were generated by a geostatistical algorithm on a regular $40 \times 120 \times 20$ Cartesian grid, as illustrated in the left plot of Figure 2.17, and then mapped onto the structural model, as shown in the plot to the right. A bit simplified, one can view the Cartesian grid model as representing the rock body at geological "time zero," when the sediments have been deposited and have formed a stack of horizontal grid layers. From geological time zero and up to now, geological activity has introduced faults and deformed the layers, resulting in the structural model seen in the left plot of Figure 2.17.

Having seen the structural model, we continue to study the petrophysical parameters. The grid cells are thought to be larger than the laminae of our imaginary reservoir, hence each grid block will generally contain both reservoir rock (with sufficient permeability) and impermeable shale. This is modeled using the net-to-gross ratio, `rock.ntg`, shown in Figure 2.18 along with the horizontal and vertical permeability. The plotting routines are exactly the same as for the porosity in Figure 2.17, but with different data and slightly different specification of the colorbar. From the figure, we clearly see that the model has a large content of shale and thus low permeability along the top, but we also see high-permeable sand bodies that cut through the low-permeable top. In general, the permeabilities seem to correlate well with the sand content given by the net-to-gross parameter.

Some parts of the sand bodies are partially covered by mud that strongly reduces the vertical communication, most likely because of flooding events. These mud-draped surfaces occur on a sub-grid scale and are modeled through a multiplier value (`MULTZ`) associated

https://doi.org/10.1017/9781108591416.004 Published online by Cambridge University Press

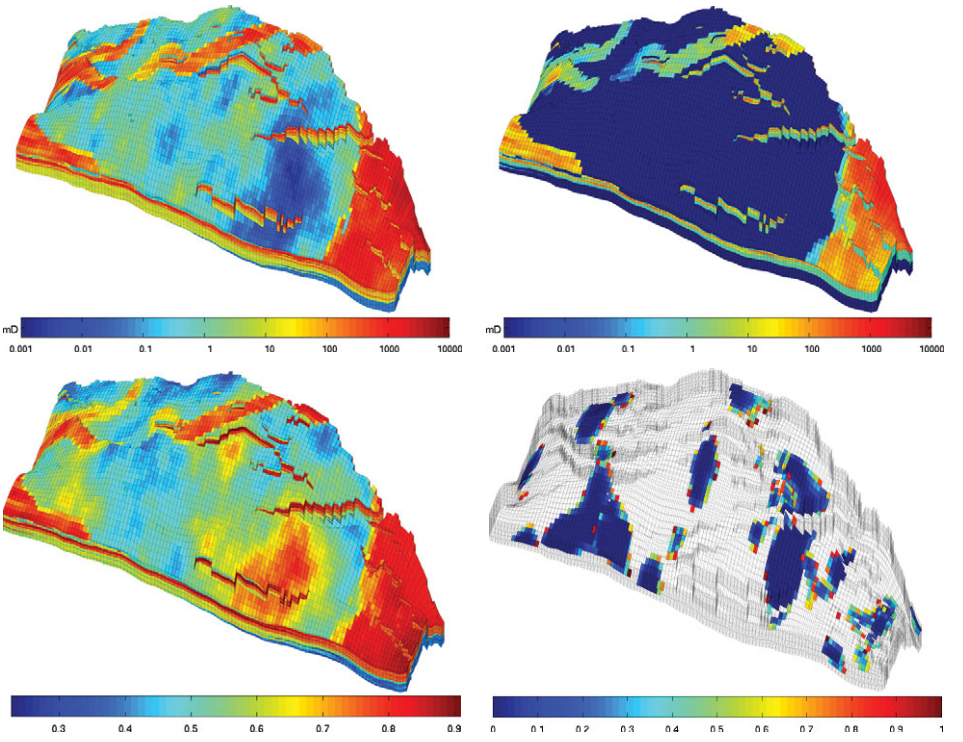

Figure 2.18 The upper plots show the permeability for the SAIGUP model, using a logarithmic color scale, with horizontal permeability to the left and vertical permeability to the right. The lower-left plot shows net-to-gross, i.e., the fraction of reservoir rock per bulk volume. The lower-right plot shows regions of the reservoir where reduced vertical communication is modeled by vertical multiplier values less than unity.

with each cell, which takes values between zero and one and can be used to manipulate the effective communication (the transmissibility) between a given cell (i, j, k) and the cell immediately above $(i, j, k + 1)$. For completeness, we remark that the horizontal multiplier values (`MULTX` and `MULTY`) play a similar role for vertical faces, but are equal one in (almost) all cells for this particular realization.

To further investigate the heterogeneity of the model, we next look at histograms of the porosity and the permeabilities, as we did for the SPE 10 example (the MATLAB statements are omitted since they are almost identical). In Figure 2.19, we clearly see that the distributions of porosity and horizontal permeability are multi-modal in the sense that five different modes can be distinguished, corresponding to the five different facies used in the petrophysical modeling.

It is common modeling practice that different rock types are assigned different rock-fluid properties (relative permeability and capillary functions), more details about such properties will be given later in the book. Different rock types are represented using the

https://doi.org/10.1017/9781108591416.004 Published online by Cambridge University Press

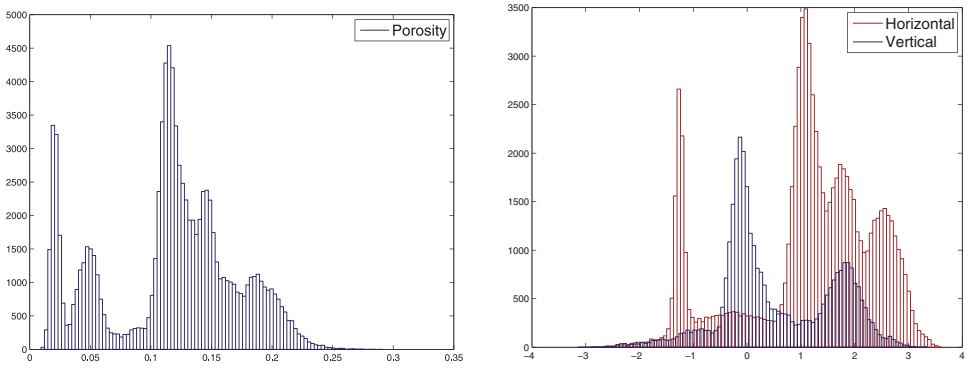

Figure 2.19 Histogram of the porosity (left) and the logarithm of the horizontal and vertical permeability (right) for the shallow-marine SAIGUP model. Since the reservoir contains five different facies, the histograms are multimodal. See also Figure 2.20.

SATNUM keyword, and by inspection of the SATNUM field in the input data, we see that the model contains six different rock types as depicted in Figure 2.20. For completeness, the figure also shows the permeability distribution inside each rock type. Interestingly, the permeability distribution is multimodal for at least two of the rock types.

Finally, to demonstrate the large difference in heterogeneity resulting from different depositional environments, we compare the realization studied so far in this example with another realization; Figure 2.21 shows porosities and rock-type distribution. Whereas the original realization corresponds to a depositional environment with a flat shoreline, the other realization has a two-lobed shoreline, giving distinctively different facies belts. The figure also clearly demonstrates how the porosity (which depends on the grain-size distribution and packing) varies with the rock types. This can be confirmed by a quick analysis:

```
for i=1:6,  pavg(i) = mean(rock.poro(SN==i));
            navg(i) = mean(rock.ntg(SN==i)); end
```

```
pavg = 0.0615    0.1883    0.1462    0.1145    0.0237    0.1924
navg = 0.5555    0.8421    0.7554    0.6179    0.3888    0.7793
```

In other words, rock types two and six are good sands with high porosity, three and four have intermediate porosity, whereas one and five correspond to less quality sand with a high clay content and hence low porosity.

Computer exercises

2.5.1 Look at the correlation between the porosity and the permeability for the SPE 10 data set. Do you see any artifacts, and if so, how would you explain them? (Hint: plot ϕ versus $\log K$.)

https://doi.org/10.1017/9781108591416.004 Published online by Cambridge University Press

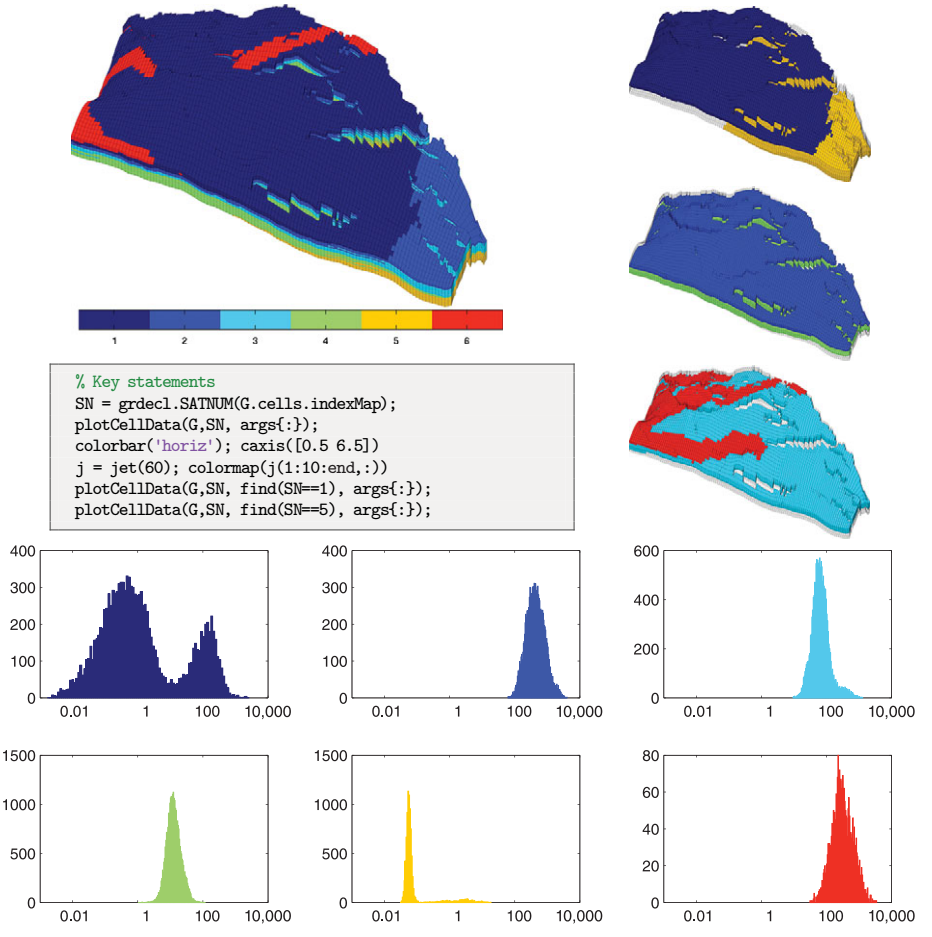

Figure 2.20 The upper-left plot shows the rock type distribution for SAIGUP. The right column shows the six rock types grouped in pairs; from top to bottom, rock types number 1 and 5, 2 and 4, and 3 and 6. The bottom part of the figure shows histograms of the lateral permeability in units [mD] for each of the six rock types found in the model.

2.5.2 Download the `CaseB4` models that represent a sector model with intersecting faults. Pick at least one model realization and set homogeneous and random petrophysical data as discussed in Sections 2.5.1 and 2.5.2.

2.5.3 The $58 \times 48 \times 10$ permeability field given in `rock1.mat` in the book module contains an unusual geological structure. Can you find what it is? (Hint: if you want to explore the model interactively, you can try to use `plotToolbar` from the `mrst-gui` module).

2.5.4 Download the `BedModels1` and `BedModel2` data sets that represent sedimentary beds similar to the facies model shown in Figure 2.7. Use the techniques introduced in Sections 2.5.3–2.5.5 to familiarize yourself with these models:

https://doi.org/10.1017/9781108591416.004 Published online by Cambridge University Press

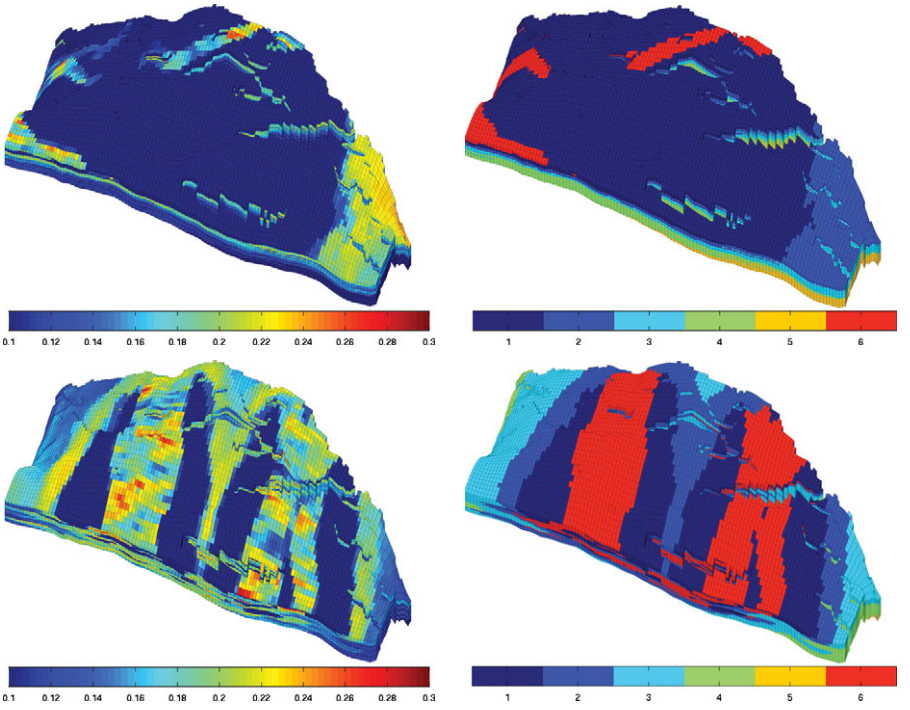

Figure 2.21 Comparison of porosity (left) and the distribution of rock types (right) for two different SAIGUP realizations.

- look at porosities and permeabilities in physical space
- compare with the same quantities in ijk space
- find models that have facies information and look at the distribution of petrophysical properties inside each facies

2.5.5 Modify the `simpleGravityColumn` example from Section 1.4 so that it uses the geometry and petrophysical data in the `mortarTestModel` or `periodic Tilted` models from the `BedModels1` data set instead. Can you explain what you observe?

https://doi.org/10.1017/9781108591416.004 Published online by Cambridge University Press